

Operator splitting for high-order adaptive mesh refinement on the sphere

Amik St-Cyr ¹

1) *NCAR 1850 Table Mesa Drive Boulder, CO 80305, USA*

Corresponding Author : Amik St-Cyr, amik@ucar.edu

ABSTRACT

A variant of the operator integrating factor splitting originally proposed by Maday et al. (1990) is applied to a h -adaptive, non-conforming spectral element shallow water model over the sphere. The resulting algorithm is efficient and avoids any type of local time-stepping like in the Berger-Oliger algorithm. The model is tested against the shallow water cases proposed by Williamson et al. (1992). The numerical results show that it is possible to keep the semi-implicit time step constant while varying the advective time scale to meet the maximal Courant restriction.

1 INTRODUCTION

The ill posedness of the primitive equations¹ for any kind of non-periodic boundary conditions, was demonstrated by Oliger and Sundstrom [7]. The classical AMR² algorithm of Berger and Oliger [1] cannot be applied directly because it involves local time-stepping. This is a severe restriction for spatially adaptive climate simulations: a problem requiring multiple, century-long integrations of the equations governing the Earth's atmosphere. The consequences on numerical methods are twofold. First, extremely efficient time-stepping algorithms need to be employed. Secondly, because of the computational resources available, global grid resolutions in atmospheric climate models are much coarser than in numerical weather models. The latter are employing much finer grids but not over the entire sphere. However, the need for finer grids in climate simulations is necessary to verify that severe weather events like hurricanes have an influence on the correct climate signal. The first numerical issue is investigated: efficient non-local time stepping for handling the primitive equations on dynamically adaptive grids. The proposed algorithm thereafter is based on the operator integrating factor (OIF) of Maday et al. [5]. Robert [8] demonstrated that a six-fold increase over the explicit time step for atmospheric general circulation models could be achieved without recourse to a fully implicit integrator. The algorithm consisted in a semi-Lagrangian treatment of advection combined with a semi-implicit scheme for the stiff terms responsible for gravity waves. Recently, St-Cyr and Thomas [12] demonstrated that the semi-implicit semi-Lagrangian approach is equivalent to the general OIF algorithm when the stiff terms are separated from the advective ones.

¹ Navier-Stokes under the shallow atmosphere and dominating vertical pressure gradient assumptions

² Adaptive Mesh Refinement

2 SHALLOW WATER EQUATIONS

The shallow water equations have been used as a vehicle for testing promising numerical methods for many years by the atmospheric modeling community. They contain the essential wave propagation mechanisms found in atmospheric general circulation models. These are the fast-moving gravity waves and nonlinear Rossby waves. The latter are important for correctly capturing nonlinear atmospheric dynamics. The governing equations of motion for the inviscid flow of a free surface are

$$\frac{\partial \mathbf{v}}{\partial t} + (f + \zeta) \hat{\mathbf{r}} \times \mathbf{v} + \nabla \left(\frac{1}{2} \mathbf{v} \cdot \mathbf{v} + \Phi \right) = 0, \quad (1)$$

$$\frac{\partial \Phi}{\partial t} + \nabla \cdot \Phi \mathbf{v} = 0. \quad (2)$$

\mathbf{v} is the horizontal velocity and $\Phi = gh$ the geopotential height where h is the height above sea level and g is the gravitational acceleration constant. The given Coriolis parameter f depends only on the position vector on the sphere and $\hat{\mathbf{r}}$ is a unit vector in the radial direction. In the above system $\zeta = \hat{\mathbf{r}} \cdot \nabla \times \mathbf{v}$ represents the component of the vorticity in the radial direction. The flux form shallow-water equations in curvilinear coordinates are described in Sadourny [9]. Let \mathbf{a}_1 and \mathbf{a}_2 be the covariant base vectors of the transformation between the cube inscribed into the sphere and the surface of the sphere. The metric tensor of the transformation is defined as $G_{ij} \equiv \mathbf{a}_i \cdot \mathbf{a}_j$. Covariant and contravariant vectors are related through the metric tensor by $u_i = G_{ij} u^j$, $u^i = G^{ij} u_j$, where $G^{ij} = (G_{ij})^{-1}$ and $G = \det(G_{ij})$. The six local coordinate systems, denoted by (x^1, x^2) for all faces, are based on equiangular central projection, $-\pi/4 \leq x^1, x^2 \leq \pi/4$. The metric tensor for all six faces of the cube is

$$G_{ij} = \frac{1}{r^4 \cos^2 x^1 \cos^2 x^2} \begin{bmatrix} 1 + \tan^2 x^1 & -\tan x^1 \tan x^2 \\ -\tan x^1 \tan x^2 & 1 + \tan^2 x^2 \end{bmatrix} \quad (3)$$

where $r = (1 + \tan^2 x^1 + \tan^2 x^2)^{1/2}$ and $\sqrt{G} = 1/r^3 \cos^2 x^1 \cos^2 x^2$. To formulate the shallow water equations in curvilinear coordinates, the spatial operators like vorticity and divergence are replaced with their curvilinear definitions namely $\zeta = \frac{1}{\sqrt{G}} \left[\frac{\partial u_2}{\partial x^1} - \frac{\partial u_1}{\partial x^2} \right]$ and $\frac{1}{\sqrt{G}} \nabla \cdot \sqrt{G} \mathbf{u}$ where \mathbf{u} denotes the covariant velocity.

3 NONLINEAR OPERATOR INTEGRATING FACTOR SPLITTING

To avoid problems related to ill-posed boundary conditions and local time stepping, we adopt the nonlinear operator integration factor splitting (OIFS) scheme developed in [12]. Sub-stepping is applied to

$$\frac{\partial \tilde{\mathbf{v}}}{\partial s} + \tilde{\zeta} \mathbf{k} \times \tilde{\mathbf{v}} + \frac{1}{2} \nabla (\tilde{\mathbf{v}} \cdot \tilde{\mathbf{v}}) = 0, \quad (4)$$

$$\frac{\partial \tilde{\Phi}}{\partial s} + \nabla \cdot (\tilde{\Phi} \tilde{\mathbf{v}}) = 0. \quad (5)$$

with initial conditions $\tilde{\mathbf{v}}(\mathbf{x}, t^{n-q}) = \mathbf{v}(\mathbf{x}, t^{n-q})$, $\tilde{\Phi}(\mathbf{x}, t^{n-q}) = \Phi(\mathbf{x}, t^{n-q})$. The integration factor $Q_S^{t^*}(t)$ is applied to the remaining de-coupled system of equations containing the Coriolis and

linear gravity wave terms

$$\frac{d}{dt} Q_S^{t^*}(t) \begin{bmatrix} \mathbf{v} \\ \Phi \end{bmatrix} = -Q_S^{t^*}(t) \begin{bmatrix} f \mathbf{k} \times \mathbf{v} + \nabla \Phi \\ \Phi_0 \nabla \cdot \mathbf{v} \end{bmatrix} \quad (6)$$

where the geopotential height is decomposed into a perturbation about a constant base state, Φ_0 . For an implicit second order backward differentiation formula (BDF-2), sub-stepping of the right-hand-side terms is not required because $Q_S^{t^n}(t^n) = I$. The resulting time discretization of (6) is given by

$$\mathbf{v}^n + \frac{2}{3} \Delta t \mathbf{N} \nabla \Phi^n = \frac{4}{3} \mathbf{N} \tilde{\mathbf{v}}^{n-1} - \frac{1}{3} \mathbf{N} \tilde{\mathbf{v}}^{n-2} \quad (7)$$

$$\Phi^n + \frac{2}{3} \Delta t \Phi_0 \nabla \cdot \mathbf{v}^n = \frac{4}{3} \tilde{\Phi}^{n-1} - \frac{1}{3} \tilde{\Phi}^{n-2} \quad (8)$$

where

$$\mathbf{N} = \left(I + \frac{2}{3} \Delta t f \mathbf{M} \right)^{-1}, \quad \mathbf{M} = \begin{bmatrix} 0 & -1 \\ 1 & 0 \end{bmatrix} \quad (9)$$

The values of the fields $\tilde{\mathbf{v}}$ and $\tilde{\Phi}$ at time levels $n - 1$ and $n - 2$ are computed by sub-stepping (4) and (5) on the intervals $[t^{n-1}, t^n]$ and $[t^{n-2}, t^n]$. An implicit equation for Φ^n is obtained after space discretization and application of block Gaussian elimination, resulting in a modified Helmholtz problem. The non-symmetric linear system is solved using the conjugate-gradient squared (CGS) algorithm. For spectral elements, the linear advection operator is skew-symmetric with purely imaginary eigenvalues. Therefore, an efficient time integration scheme for sub-stepping should have a stability region that includes a large portion of the imaginary axis. A fourth-order Runge-Kutta (RK-4) scheme is employed for sub-stepping. The shallow water equations are discretized in space using the $\mathbb{P}_N - \mathbb{P}_{N-2}$ spectral element method (see [13]).

4 SPECTRAL ELEMENT DISCRETIZATION

The equations of motion are discretized in space using the $\mathbb{P}_N - \mathbb{P}_{N-2}$ spectral element method as in [13]. The cubed-sphere is partitioned into K elements Ω^k in which the dependent and independent variables are approximated by tensor-product polynomial expansions. The velocity is expanded in terms of the N -th degree Lagrangian interpolants h_i and the geopotential is expanded using the $(N - 2)$ -th degree interpolants \tilde{h}_i :

$$\mathbf{v}_h^k(r_1, r_2) = \sum_{i=0}^N \sum_{j=0}^N \mathbf{v}_{ij}^k h_i(r_1) h_j(r_2), \quad \Phi_h^k(r_1, r_2) = \sum_{i=1}^{N-1} \sum_{j=1}^{N-1} \Phi_{ij}^k \tilde{h}_i(r_1) \tilde{h}_j(r_2).$$

A weak Galerkin formulation results from integration of the equations with respect to test functions and direct evaluation of inner products using Gauss-Legendre and Gauss-Lobatto-Legendre quadrature. C^0 continuity of the velocity is enforced at inter-element boundaries sharing Gauss-Lobatto-Legendre points by applying a direct stiffness summation [2]. The advection operator in the momentum equation is then expressed in terms of the relative vorticity and kinetic energy, whereas the continuity equation relies on the velocity form. Wilhelm and Kleiser

[14] have shown that the rotational form of the advection operator is stable for the $\mathbb{P}_N - \mathbb{P}_{N-2}$ spectral element discretization.

4.1 Non-conforming elements

The collocation points at the boundaries of non-conforming spectral elements are not coincident and a procedure is required to glue these elements together. Several techniques are available including mortars [6], and interpolation [3]. The true unknowns at a boundary belong to the master coarse element and are passed to the refined slave elements by a procedure described in what follows. From (10), at one of the element boundaries Γ_{km} where $r_1 = 1$, the trace of the solution is

$$\mathbf{v}(r_1, r_2)_h^k|_{\Gamma_{km}} = \mathbf{v}_h^k(r_2) = \sum_{j=0}^N \mathbf{v}_{Nj}^k h_j(r_2) \quad (10)$$

where h_j are the Lagrange interpolants defined at the Gauss-Legendre-Lobatto (GLL) points. To interpolate the master solution to the slave edge, a mapping is created from the slave reference element relative to the master's reference element. Let η_m^l denote this mapping where $m \in [1, 2^l]$ is the slave face number and l is the level of h -refinement. Interpolation can be expressed in matrix form as

$$\left[J_m^l \right]_{ij} = h_j(\eta_m^l(\xi_i)) \quad (11)$$

where $\{\xi_i\}_{i=0}^N$ are the Gauss-Legendre-Lobatto points used in the quadrature and in the collocation of the dependent variables. If \mathbf{v}^k are the unknowns on the edge of the master element, then $J_m^l \mathbf{v}^k$ represents the master element contributions passed to the slave elements. Assembly of the global spectral element matrix is not viable on today's computers. The action of the assembled matrix on a vector is performed with the help of a direct stiffness summation (DSS). For A , a matrix resulting from the spectral element discretization of a differential operator, defined for the true degrees of freedom and A_L , the block diagonal matrix of the individual local contributions of each element as if they were disjoint, the DSS for conforming elements is represented by

$$v^T A u = v^T (\tilde{Q}^T J_L^T) A_L (J_L \tilde{Q}) u = v^T Q^T A_L Q u \quad (12)$$

where a non-conforming formulation can be obtained by replacing the scattering boolean matrices \tilde{Q} with $Q = J_L \tilde{Q}$. The block diagonal matrix J_L consist of the identity where the interface between elements are matching and of the interpolation matrix (11) where interfaces are non-conforming.

5 NUMERICAL EXPERIMENTS

Our numerical experiments are based on the shallow water test suite of Williamson et al (1992) and are well suited to asses the quality of numerical algorithms for climate modeling.

Stationary geostrophic flow: Test case 2 is a stationary East-West flow, representing a balance between the Coriolis and geopotential gradient forces in the momentum equation. The velocity

field on the sphere is specified initially (and for all time) as

$$u = u_0 (\cos \theta \cos \alpha + \cos \lambda \sin \theta \sin \alpha), \quad v = -u_0 \sin \lambda \sin \alpha .$$

where α is the angle between the axis of solid body rotation and the polar axis. The angles θ and λ are the latitude and longitude respectively. The analytic geopotential field $\Phi = gh$ is specified as

$$\Phi = \Phi_0 - \left(a\Omega u_0 + \frac{u_0^2}{2} \right) \times (-\cos \lambda \cos \theta \sin \alpha + \sin \theta \cos \alpha)^2 .$$

a is the radius of the earth and Ω is the rotation rate. Parameter values are specified to be $u_0 = 2\pi a/(12\text{days})$ and $\Phi_0 = 2.94 \times 10^4 \text{ m}^2/\text{s}^2$. The Coriolis parameter associated with this solution is $f = 2\Omega (-\cos \lambda \cos \theta \sin \alpha + \sin \theta \cos \alpha)$. This is a difficult test for the nonlinear OIFS scheme because sub-stepping is active even when the solution is stationary. The purpose of the test is to determine if BDF-2/RK-4 time stepping performs better than a Crank-Nicholson/Leap-frog (CNLF) scheme under p and h refinement. A large time step size was chosen ($dt = 1200s$), representing the time scale of physical processes. The BDF-2/RK-4 integrator enables the model to refine one level deeper with respect to h or p while maintaining the same time step size.

Elements:	6^2 GLL	8^2 GLL	10^2 GLL	16^2 GLL
24	SI/OIFS	SI/OIFS	SI/OIFS	SI/OIFS
96	SI/OIFS	SI/OIFS	SI/OIFS	failed/OIFS
384	SI/OIFS	SI/OIFS	failed/OIFS	
1536	SI/OIFS	failed/OIFS		
6144	failed/OIFS			

Table 1 Robustness test for OIFS and CNLF time stepping for test case 2. Failed indicates when the time-stepping scheme becomes unstable.

Flow over a mountain: Test case 5 is a zonal flow impinging on a mountain. The mean equivalent depth of the atmosphere is set to $h_0 = 5960$ meters. The mountain height is given by $h_s = h_{s_0}(1 - r/R)$, where $h_{s_0} = 2000$ m, $R = \pi/9$, and $r^2 = \min[R^2, (\lambda - \lambda_c)^2 + (\theta - \theta_c)^2]$. The center of the mountain is located at $\lambda_c = 3\pi/2$ and $\theta_c = \pi/6$ in spherical coordinates. An exact solution is not known and relative error metrics are computed by comparing against a T213³ spectral transform reference solution. The problem is integrated for 15 days with a base mesh of resolution 5 degrees. Three levels of static refinements where the mountain height is greater than $0m$. In addition, dynamic refinements with 3 refinement levels are applied where the absolute value of the relative vorticity is greater than $2e - 5s^{-1}$ (see [11]). Numerical simulations demonstrate that the semi-implicit time step can be kept constant while changing the CFL condition of the OIF problem related to the advective scales: this leads to an efficient method for AMR simulations. Figure 1 shows the solution after 15 days.

REFERENCES

1. Berger, M. and J. Oliger, 1984: Adaptive mesh refinement for hyperbolic partial differential equations. *J. Comput. Phys.*, **53**, 484–512.

³ A 640×320 Global Gaussian grid on the sphere in spherical coordinates.

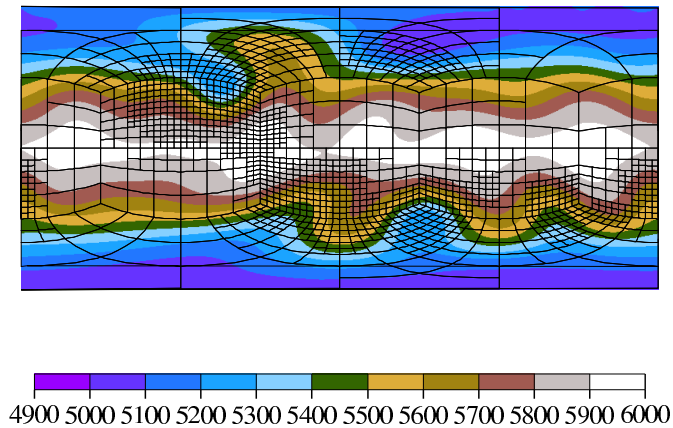


Figure 1. Plot of the geopotential height at 5 days for the flow impinging a mountain.

2. Deville, M. O., Fischer, P. F., and Mund, E. H., 2002: High-Order Methods for Incompressible Fluid Flow. Cambridge monographs on applied and computational mathematics. Cambridge University Press, 2002.
3. Fischer, P. F., G.W. Kruse, and F. Loth, 2002: Spectral element methods for transitional flows in complex geometries. *J. Sci. Comput.*, **17**, 81–98.
4. Kwizak, M., and A. J. Robert, 1971: A semi-implicit scheme for grid point atmospheric models of the primitive equations. *Mon. Wea. Rev.*, **99**, 32–36.
5. Maday, Y., A. T. Patera, and E. M. Ronquist, 1990: An operator-integration-factor splitting method for time-dependent problems: Application to incompressible fluid flow. *J. Sci. Comput.*, **5**, 263–292.
6. Mavriplis, C., 1989: *Nonconforming Discretizations and a Posteriori Error Estimators for Adaptive Spectral Element Techniques*, Ph. D. thesis, MIT, 1989.
7. Olinger, J. and A., Sundstrom, 1978: Theoretical and practical aspects of some initial boundary value problems in fluid dynamics. *SIAM J. Appl. Math.*, **35**, 419–446.
8. Robert, A. J., 1981: A stable numerical integration scheme for the primitive meteorological equations. *Atmos.-Ocean*, **19**, 35–46.
9. Sadourny, R., 1972: Conservative finite-difference approximations of the primitive equations on quasi-uniform spherical grids. *Mon. Wea. Rev.*, **100**, 136–144.
10. Staniforth, A. N., and H. J. Mitchell, 1977: A semi-implicit finite-element barotropic model. *Mon. Wea. Rev.*, **105**, 154–169.
11. St-Cyr, A., J.M., Dennis, C., Jablonowski, S.J. Thomas and H.M. Tufo, 2006: A Study of Adaptive Non-Conforming GCMs for Climate Modeling. Submitted to *Month. Wea. Rev.* .
12. St-Cyr, A., and S. J. Thomas, 2005: Nonlinear operator integration factor splitting for the shallow water equations. *Appl. Numer. Math.*, **52**, No. 4, 429-448.
13. Thomas, S. J., and R. D. Loft, 2002: Semi-implicit spectral element atmospheric model. *J. Sci. Comp.*, **17**, 339–350.
14. Wilhelm, D., and Kleiser, L., 2000: Stable and unstable formulation of the convection operator in spectral element simulations. *Appl. Numer. Math.* **33**, 275–280.
15. Williamson, D. L., J. B. Drake, J. J. hack, R. Jakob, P. N. Swarztrauber, 1992: A standard test set for numerical approximations to the shallow water equations in spherical geometry *J. Comp. Phys.*, **102**, 211–224.